Pergamon

Tetrahedron 57 (2001) 9415–9422

TETRAHEDRON

Electron density analysis of small ring ethers

Antonio Vila[a] and Ricardo A. Mosquera[b,*]

[a]*Departamento de Física Aplicada, Facultade de Ciencias, Universidade de Vigo, Campus de Ourense, 32004 Ourense, Galicia, Spain*
[b]*Departamento de Química Física, Facultade de Ciencias, Universidade de Vigo, Campus de Vigo, Lagos-Marcosende s/n, 36200 Vigo, Galicia, Spain*

Received 14 June 2001; revised 27 August 2001; accepted 25 September 2001

Abstract—Atoms in molecules theory (AIM) was employed to compute the atomic properties for a series of five protonated and neutral oxacycloalkanes $(CH_2)_nO$ (n=2–6), on B3LYP/6-311++G(2d,2p) electron distributions. Atomic energies indicate that strain of oxacycloalkanes results from a destabilization of oxygen and hydrogens that is not compensated for by the stabilization of cyclic carbons. Atomic electron populations point out that cycloalkyloxonium cations are better described by an $O–H^+$ structure than by the widespread use of the $O^+–H$ structure.

1. Introduction

In contrast to the large number of topological studies on three membered rings (see Refs. 1–5, among others), the electron density studies on larger rings containing heteroatoms, have received little attention.

The present work continues our research into the electron density properties of alkyl ethers. Our previous work focused on the evaluation of transferability in linear ethers;[6] protonation on linear ethers,[7] stepwise fluorination on dimethoxymethane;[8,9] dimerization of dimethoxymethane;[10] and the topological analysis of substituted oxacyclopropane.[11] The main purpose of this work is to obtain a theoretical understanding of the properties of small ring ethers, and their protonated forms, within the framework of the atoms in molecules theory (AIM).[12,13] Especially, we aim to analyze the changes in atomic and bond properties due to the ring formation, and the relationships between those modifications and the ring strain energy, E_{RS}.[14]

In the earliest approaches, based on a certain group additivity scheme,[15] the strain energy was estimated as the difference from the heat of formation of the test molecule and that of a hypothetical strainless reference. The scarcity of heats of formation prompted the employment of heats of appropriately chosen chemical reactions. Thus, homodesmotic reactions[16] which preserve the valence environment around each atom in the test molecule, are widely employed in evaluating ring strain. Nevertheless, the definition of E_{RS} is still a point of controversy in the chemical literature and it has to be borne in mind that no definition hitherto proposed can be considered as generally accepted. Also, E_{RS} has been ascribed to diverse origins, though without a rigorous physical basis.

The development of the AIM theory and its associated unique definition for an atom in a molecule provided the physical basis for understanding E_{RS}. Thus, the strain energy of small cycloalkanes was quantitatively ascribed to the balance between increased stability of the C atoms and hydrogen destabilizations with respect to a standard methylene group of a linear n-alkane. These changes in the atomic energies were explained by electron charge transfers from hydrogen to carbon atoms, due to the enhanced electronegativity of carbon in a cycle, enhancement predicted by the hybridization model as a consequence of geometry modifications.[13,17] In spite of its successful explanation of E_{RS} in cycloalkanes, no similar studies with the AIM theory were carried out on small heterocycles.

2. Theory of atoms in molecules and computational technique

The AIM theory put forward by Bader and collaborators allows the calculation of atomic properties by integration of the proper density function within regions, Ω, bounded by a zero flux surface for the gradient of the charge vector field, which can be identified with molecular atoms (see Ref. 12 and references cited therein). The discussion performed in this work is based on the calculation of the electron atomic population of an atom $N(\Omega)$ and its energy $E(\Omega)$. The AIM theory also defines major elements of molecular structure in terms of the properties of critical points in the electron density ρ. Along the path defined by the maximum electron density line (MEDL) connecting two bonded atoms

Keywords: ab initio calculations; AIM theory; cyclic ethers; protonation.
* Corresponding author. Tel.: +34-986912298; fax: +34-986812382; e-mail: mosquera@uvigo.es

0040–4020/01/$ - see front matter
PII: S0040-4020(01)00946-2

Table 1. Total energies, virial ratio (γ), vibrational energies (ZPVE), errors in the integrated energies and populations for various cyclic ethers $(CH_2)_nO$ as obtained from B3LYP/6-311++G(2d,2p) wave functions

		E (a.u.)	ZPVE (kJ mol^{-1})	$E-\sum E(\Omega)$ (kJ mol^{-1})	γ	$N-\sum N(\Omega)$ (a.u.)	$\sum L(\Omega($ (a.u.)
1	$(CH_2)_2O$	−153.84181	150.24	−0.05	2.00392	−0.0001	−0.0002
1+	$(CH_2)_2OH^+$	−154.14614	184.44	0.89	2.00387	0.0003	0.0006
2	$(CH_2)_3O$	−193.17190	227.69	−0.33	2.00412	0.0010	0.0014
2+	$(CH_2)_3OH^+$	−193.49516	262.91	1.91	2.00410	0.0018	0.0025
3	$(CH_2)_4O$	−232.52816	305.76	2.16	2.00424	0.0032	0.0031
3+	$(CH_2)_4OH^+$	−232.85570	340.60	3.27	2.00423	0.0037	0.0046
4	$(CH_2)_5O$	−271.86043	383.61	3.44	2.00434	0.0049	0.0054
4+	$(CH_2)_5OH^+$	−272.18881	417.98	2.74	2.00434	0.0044	0.0052
5	$(CH_2)_6O$	−311.17322	458.29	1.37	2.00441	0.0020	0.0017
5+	$(CH_2)_6OH^+$	−311.50423	495.99	2.58	2.00436	0.0038	0.0042

there exists a critical point for the charge density, termed a bond critical point (BCP). Whenever a set of bonded atoms form a cycle, a ring critical point (RCP) appears as a topological consequence. Properties of interest at the BCP and RCP critical points are: electronic charge density, ρ; and laplacian of the charge density $\nabla^2\rho$. Another property of interest at BCPs is the bond ellipticity, defined as $\epsilon=(\lambda_1/\lambda_2-1)$, where λ_1 and λ_2 are, respectively, the largest and the smallest of the two curvatures of the charge density perpendicular to the bond path. Hereafter, local properties at BCP and RCP are designated by the subscripts b and r, respectively.

DFT calculations on the five smallest oxacycloalkanes and their protonated forms were carried out using the Gaussian 94 quantum chemical suite of programs[18] at the B3LYP/6-311++G(2d,2p) level. The evaluation of all local properties was performed using MORPHY98.[19] The integrations over the atomic basins were carried out using the AIMPAC program series.[20] Interatomic surfaces were determined by employing the more accurate PROMEGA surface algorithm, searching up to three intersections between a given ray originated at the nucleus and the interatomic surface, and employing a total amount of 720000 quadrature points per atomic basin.

3. Results and discussion

Table 1 displays the calculated B3LYP/6-311++G(2d,2p) energies, virial ratios (defined as $\gamma=-V/T$, where V is the electronic potential energy and T the electronic kinetic energy) and integration errors expressed as differences between total properties and those obtained by summation of properties of the fragments [$N-\sum N(\Omega)$or $E-\sum E(\Omega)$] and as the summation of the integrated values of the laplacian of the charge density in all the atomic fragments [$\sum L(\Omega)$]. If compared with previous work at similar theoretical levels,[8,9,11] the discrepancies in the additivity of atomic charges and energies from their molecular counterparts, are found to be significantly improved. Although in this case $L(\Omega)$ values have been significantly reduced by increasing the amount of quadrature points in the atomic basin, it has to be borne in mind that in general, integration error function and this number display an erratic relationship.[21]

3.1. Structures and bonding

We have restricted our attention to the most stable conformer in each compound, according to previous conformational studies.[22–24] Thus, the geometry of the oxacyclobutane was optimized from an initial conformation with a non-planar ring. This gave rise to a final C_{2v} planar structure, whereas a slightly puckered structure was proposed in a previous X-ray study.[25] The planar structure was confirmed to be a local minimum, since all its frequencies are real. The lowest B3LYP frequency (66.5 cm^{-1}) is undoubtedly assigned to the ring puckering vibration.

The C_s chair conformers of oxacyclopentane, and oxacyclohexane were also characterized as minima. An approximately twist-boat conformation of oxacycloheptane was confirmed as a minimum at this computational level.

Local properties at C–O bond critical points are listed in Table 2, along with the charge density at the RCP. The B3LYP/6-311++G(2d,2p) C–O bond lengths in structures **1** and **2** mirror quite closely their experimental counterparts (R_{C-O}(**1**)=1.431 Å, and R_{C-O}(**2**)=1.449 Å).[26] The agreement

Table 2. Electron density local properties at O–C bond critical points and ring critical points. Distances in angstroms and the remaining properties in a.u.

Compound	R_{C-O}	ΔR_{C-O}	ρ_b	$\nabla^2\rho_b$	ϵ	ρ_r	η
1	1.4323	0.0021	0.2514	−0.4571	0.4963	0.2058	81.40
1+	1.5309	0.0536	0.1899	−0.0493	1.0505	0.1748	80.18
2	1.4504	0.0002	0.2505	−0.6254	0.03397	0.0901	36.57
2+	1.5432	0.0041	0.1809	−0.2112	0.03701	0.0796	39.38
3	1.4357	0.0011	0.2524	−0.6209	0.03245	0.0433	17.34
3+	1.5388	0.0013	0.1804	−0.2113	0.03067	0.0386	18.82
4	1.4246	0.0008	0.2580	−0.6418	0.01951	0.0211	8.30
4+	1.5262	0.0006	0.1848	−0.2203	0.01135	0.0185	8.90
5	1.4243	0.0010	0.2583	−0.6355	0.00443	0.0131	5.17
5+	1.5433	0.0006	0.1773	−0.2015	0.04254	0.0111	5.83

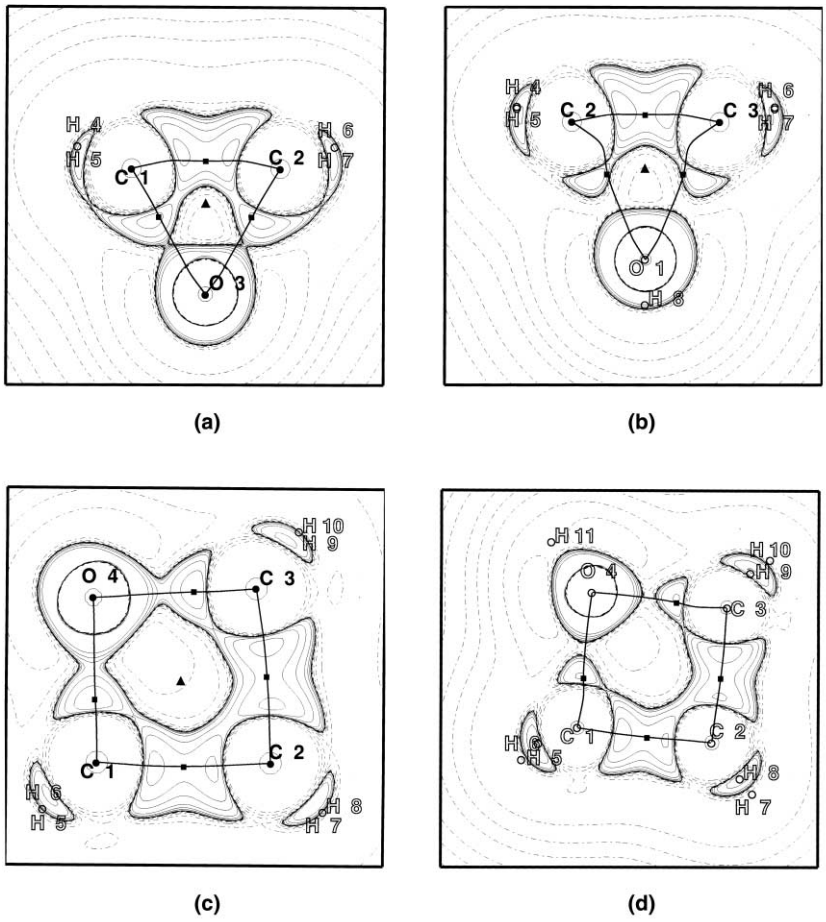

Figure 1. (a) Contour maps of the Laplacian of the charge density for oxacyclopropane, (b) protonated oxacyclopropane, (c) oxacyclobutane, and (d) protonated oxacyclobutane. Dotted contour corresponds to 0 a.u. Solid contours are for regions of local charge concentration ($\nabla^2\rho<0$) and dashed lines for regions of local charge depletion ($\nabla^2\rho>0$). The contours ($\times10^3$ a.u.) for both $\pm$ values are: 2, 4, 8, 20, 40, 80, 200, 400, 800. Bondpaths are bold lines, charge density BCPs are indicated with squares, triangles represent charge density RCPs. Circles represent nuclei (bold type in-plane, and open face are projections of out of plane).

with the experimental geometry is only slightly worse for compound **3** (R_{C-O}(**3**)=1.430 Å).[27]

Though empirical relationships between ρ_b and bond length have been found for several covalent bonds along diverse homologous series,[12,28–30] the bond lengths of cyclic compounds depend more on how the cycle can be formed with minimum strain energy than on the ρ_b values.[11] Thus, that kind of relationships cannot be established along the series here considered.

The difference between the length of the MEDL connecting two bonded nuclei and the corresponding geometrical distance, ΔR, is also provided in Table 2. We observe that the curvature of the C–O MEDL is only significant for compounds **1**+ and **2**+. On the other hand, C–C MEDLs are noticeably curved in compounds **1** and **2** (about 0.02 a.u. in both compounds). Thus, though all the bonds of a small cycloalkane are substantially curved, the C–C bonds are the only ones affected in small oxacycloalkanes. The opposite trend was found for phosphirane and phosphetane where C–P MEDL were more bent than the C–C ones.[31] As it was reported in previous works performed at different computational levels[1,11] the protonation of oxacyclopropane results in a change from an outwardly curved structure to an inwardly one. On the other hand protonation of oxacyclobutane transforms a slightly outwardly structure into another where the only inwardly MEDL are those connecting C^α atoms with the corresponding C–O BCP (Fig. 1). Protonation of oxacyclobutane also gives rise to ring puckering, yielding a C_s structure for **2**+.

The ellipticity at C–O BCPs displays very high values in **1** and **1**+ that are in contrast to the remaining compounds. This is a consequence of the smooth rate of fall off experienced by the charge density in any direction parallel to the ring surface (the values of the two negative curvatures for **1** are −0.4899 and −0.3274 a.u., respectively). This fact and the relatively high value (81.4%) of the ratio, η, between the charge density at the RCP, ρ_r, and the average of the charge density at the peripheral BCPs (Table 2) reflect that the charge density is highly delocalized over the entire surface of the ring in oxacyclopropane. This feature, termed σ-delocalization,[1,2] is a characteristic of three membered rings. In fact, η ratio dramatically declines (according to an exponential relationship) as the ring increases in size (Fig. 2). The Laplacian of the charge density, that provides for every point a measure of the local charge concentration (negative values) or depletion (positive values), can also be employed to monitor the decrease of charge accumulation

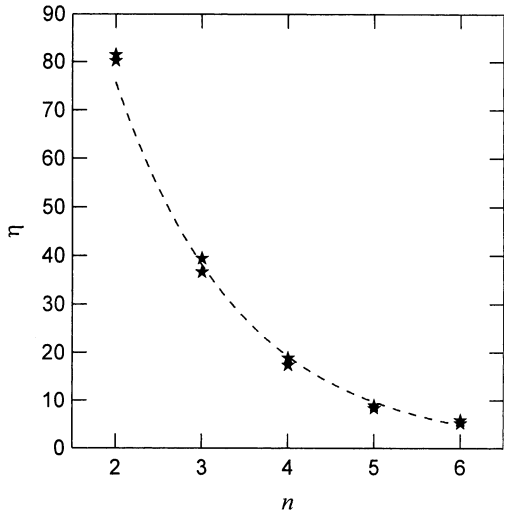

Figure 2. Plot of the electron density surface delocalization index (η) vs. the number of methylene groups (n) in the ring. See text for further details.

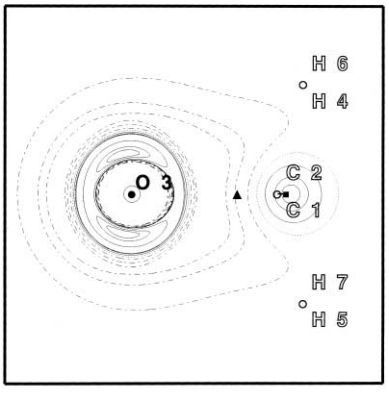

(a)

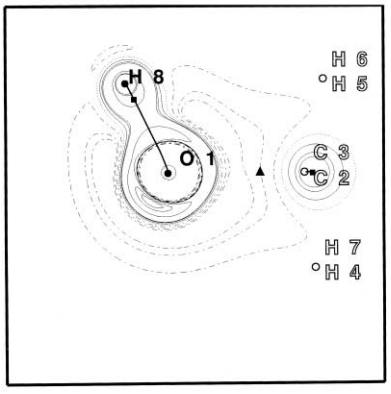

(b)

Figure 3. (a) Contour maps of the Laplacian of the charge density for the perpendicular plane bisecting the molecule, in oxacyclopropane, and (b) protonated oxacyclopropane. Dotted contour corresponds to 0 a.u. Solid contours are for regions of local charge concentration ($\nabla^2\rho<0$) and dashed lines for regions of local charge depletion ($\nabla^2\rho>0$). The contours ($\times 10^3$ a.u.) for both $\pm$ values are: 0.2, 0.4, 0.5, 2.0, 4.0, 5.0. Bondpaths are bold lines, charge density BCPs are indicated with squares, triangles represent charge density RCPs. Circles represent nuclei (bold type in-plane, and open face are projections of out of plane).

Table 3. Electron population (a.u.) of the skeletal atomic basins in neutral oxacycloalkanes

Compound	N(O)	N(Cα)	N(Cβ)	N(Cγ)
1	8.7775	5.6020		
2	8.9528	5.5219	5.9550	
3	8.9887	5.5060	5.9358	
4	9.0129	5.4880	5.9305	5.9261
5[a]	9.0171	5.4856	5.9335	5.9243
		5.4868	5.9389	5.9184

[a] Two values are given for each position because of C_1 symmetry.

Table 4. p character for the sp^n hybrid orbitals corresponding to the different C–H bonds in oxacycloalkanes

Compound	n(C$^\alpha$–H)	n(C$^\beta$–H)	n(C$^\gamma$–H)
1	2.03		
2	2.62	2.76	
3	2.65	2.94	
4	2.74	3.05	3.13
5	2.80	3.32	3.22

Computed from H–C–H inter-bondpath angles, θ, by using $n=-\sec\theta$.

inside the ring, on going from oxacyclopropane to oxacyclobutane (Fig. 1).

Protonation does not significantly alter the conformation of the cycle if we exclude molecules **1**+, that possesses a C_s structure with a non planar ring, and **5**+. As with acyclic ethers,[7] we observe that protonation leads to stretched C(α)–O bonds (0.099, 0.093, 0.103, 0.102, and 0.119 Å), whereas the C(α)–C(β) bonds are shortened 0.013 Å by average (data not shown). Accordingly, in the corresponding protonated compound, the charge density at C–O BCPs decreases and the Laplacian becomes less negative. It is also important to notice that the index of charge delocalization inside the ring remains nearly unchanged after protonation. Fig. 3 displays the evolution of the laplacian of the charge density in the perpendicular plane that bisects the molecule after protonation of oxirane. It can be observed that the nonbonded charge concentration on oxygen is only slightly modified by protonation. In fact, $\nabla^2\rho(\mathbf{r})$ at the nonbonded (3,+3) critical point presents a value of −5.677 a.u. in **1**+ (placed at 0.366 Å from the nucleus) and −5.746 a.u. in **1** (placed at 0.338 Å from the nucleus).

3.2. Integrated atomic populations and energies

According to the hybridization model,[32] the larger H–C–H bond angles, the larger the s character of the associated C–H bonds and therefore the larger the electronegativity of the carbon with respect to the attached hydrogens. Thus, N(C) values along the series of cyclic compounds here studied are expected to display significant variations. All the H–C–H (C being C$^\alpha$, C$^\beta$, or C$^\gamma$) interpath bond angles experience a continuous closing from oxacyclopropane to oxacycloheptane (Table 3). This implies that s character of C–H bonds decreases in the same way, and explains why the electron populations of every carbon atom decrease from compound **1** to **5** (Table 4).

N(O) values monotonically increase from **1** to **5** (Table 4). This can be explained by taking into account that a larger

Table 5. Atomic energy (kJ mol^{-1}) of the skeletal atoms in the neutral species relative to that for the homologous atoms in butoxybutane

Compound	O	C(α)	C(β)	C(γ)	CH_2(α)	CH_2(β)	CH_2(γ)
1	462.1	−135.2			−25.7		
2	319.0	−23.1	5.6		17.1	26.0	
3	221.6	−16.3	19.2		3.4	23.6	
4	109.5	1.3	15.2	−19.2	27.1	12.6	−5.5
5	59.9	8.4	10.2	7.4	26.3	−17.6	8.4

B3LYP/6-311++G(2d,2p) atomic energies (in au) for butoxybutane are: $E(O)=-75.8824$, $E(C^{\alpha})=-37.7658$, $E(C^{\beta})=-38.0397$, $E(C^{\gamma})=-38.0052$, $E(C^{\alpha})=-37.7658$.

number of methylene groups in the cycle provides a wider source for electron withdrawal. As the cycle becomes larger $N(O)$ approaches its value in a open chain dialkylether. Thus $N(O)$ in oxacycloheptane (9.017 a.u.) is close to its value in butoxybutane (9.028 a.u. at the same computational level), which can be considered a good estimation for the nearly transferable value of $N(O)$ in dialkylethers.[6]

$E(O)$ values indicate that the oxygen atom is always destabilized with respect to butoxybutane (Table 5). Nevertheless, it has to be borne in mind that atomic energies cannot be compared directly between two molecules if any of them includes an heteroatom.[6,33] This is due to the strong dependence on the molecular size (measured by the summation of the nuclear charges, Z) displayed by atomic energies along any homologous series other than hydrocarbons or silanes.[34] In linear unbranched ethers this dependence gives rise to differences like 72.2 kJ mol^{-1} in $E(O)$ between methoxypropane and methoxydecane,[6] or 34.7 kJ mol^{-1} in the energy of the methyl group that is α to the oxygen in both molecules.[35]

The evolution of $E(O)$ with Z in cyclic compounds is opposite to that followed by linear molecules. It can be observed (Table 5) that the oxygen atom results stabilized by increasing Z. This is not only due to a reduction of the strain energy, because the same trend is also observed when Z is increased in alkyl substituted oxacyclopropanes.[11] Both facts are on keeping with the larger electron population of the oxygen atom in the largest oxacycloalkanes and in the largest alkyl substituted oxacyclopropanes.

On the contrary, the carbon that are α to the oxygen are monotonically destabilized when the size of the cycle increases (Table 5). Once more, it can be related to the variation in the electron population.

Protonation process is accompanied by a substantial modification of the charge distribution in all the molecules. In spite of being bonded to the proton, the changes experienced by the atomic populations of the oxygen atoms, $\Delta N(O)=N_{MH+}(O)-N_M(O)$, are always smaller than those in carbons and hydrogens (Table 6). It can be observed that, as was obtained for linear ethers,[7] the positive charge of the molecules is partially concentrated on the proton (more than its 64%) and partially dispersed over the whole molecule. The majority of the charge dispersal takes place over the hydrogens, whose atomic electron populations are reduced in the range of 0.136 a.u. (one of the hydrogens bonded to each of the C^{α} in **1**) to 0.015 a.u. (one of the hydrogens bonded to one of the C^{γ} in **5**). These facts suggests that: (a) cycloalkyloxonium cations are better described by an $O–H^+$ structure than by the widespread use of the $O^+–H$ structure; and (b) the ability of hydrogen atoms to lose electron charge during protonation. Likewise, it was found that an excess of negative charge is dispersed over the hydrogen atoms.[36,37]

Table 6. Variations experienced by atomic populations (a.u.) upon protonation

Compound	$\Delta N(O)$	$\sum\Delta N(C)$	$\sum\Delta N(H)$[a]	$N(H+)$
1	−0.0095	0.1782	−0.5092	0.3402
2	−0.0056	0.2526	−0.5987	0.3511
3	−0.0257	0.3300	−0.6554	0.3507
4	−0.0387	0.3536	−0.6800	0.3577
5	−0.0419	0.3783	−0.7039	0.3545

[a] Summation applies to all the hydrogens in the molecule but that attached to the oxygen after protonation.

Table 7. Variation of the atomic energies (kJ mol^{-1}) upon protonation

Compound	O	C^{α}	C^{β}	C^{γ}	(H)[a]
1	−94.5	−201.6			557.0
2	−178.5	−217.9	15.7		643.5
3	−125.0	−268.6	−0.5		714.1
4	−64.3	−286.7	−4.2	−8.4	723.1
5	−12.6	−310.9	−6.3	−31.2	770.3

[a] Summation of the variations experienced by the hydrogen atoms in the molecule. The hydrogen attached to the oxygen after protonation has been excluded.

The stabilization experienced by the molecule upon protonation is concentrated on the cycle (C^{β} in **2** excluded) and the attached proton, whereas the remaining hydrogens are significantly destabilized (Table 7). It can be observed that the largest stabilizations upon protonation always take place in oxygen and C^{α}. The stabilization of the oxygen atom diminishes as the number of members in the cycle increases. At the same time $\Delta E(C^{\alpha})$ becomes more negative. Both facts are again related to the evolution displayed by $\Delta N(\Omega)$ in the series.

3.3. Protonation energies

The theoretical protonation energies have been obtained as the energy difference (ΔE) between the protonated (MH^+) and neutral (M) forms. The binding energies defined in this way are affected by the basis set superposition error (BSSE), because the basis functions centered in the proton may be used in the wave function of its neutral precursor, therefore lowering its molecular energy. The BSSE has been estimated by the Boys–Bernardi's counterpoise method.[38] A theoretical proton affinity, PA_{calc},[39] is obtained after ZPVE (unscaled) and BSSE correction.

Table 8 shows the theoretical PA values, PA_{calc}, and their components, ΔE, ΔZPVE and BSSE, together with the experimental PA_{exp} values, for comparison.[40] PA_{calc} values agree to within 10.8 kJ mol^{-1} of the experimental values, which supports the reliability of theoretical energies at this level of calculation as acceptable indices in gas-phase chemistry.

Table 8. Binding energies (ΔE); vibrational energy corrections (ΔZPVE); basis set superposition error (BSSE); theoretical (PA_{calc}) and experimental (PA_{exp}) proton affinities; charges and energies on the proton at the B3LYP/6-311++G(2d,2p) level. Energies in kJ mol^{-1} and charges in au

Complex	ΔE	ΔZPVE	BSSE	PA_{calc}	PA_{exp}	$q(H^+)$	$E(H^+)$
1+	−799.02	34.20	1.29	763.53	774.2	0.6598	−822.76
2+	−848.72	35.22	1.37	812.13	801.3	0.6489	−872.72
3+	−859.96	34.84	1.23	823.89	822.1	0.6493	−874.82
4+	−862.16	34.37	0.53	827.26	822.8	0.6423	−887.42
5+	−869.07	37.70	1.20	830.17	834.2	0.6455	−891.09

In no case the protonation results in ring-opening, on the contrary of what is found for alkyl substituted oxacyclopropanes.[11,41] It is also noteworthy the gap between the protonation energy of oxacyclopropane and that for larger oxacycloalkanes, which contrasts to the continuous evolution displayed in linear dialkyl ethers.[7]

The AIM integrated electronic energy on the proton is also included in Table 8. As can be seen, this energy exceeds (<10%) the theoretical protonation energy, playing a leading role in the process. As it was commented above, protonation results in a considerable built-up of positive charge on the attached proton. We also confirm here the empirical relationships between the protonation energies and the charge on the attached proton, previously described in the chemical literature.[7,42] It suggests a dominant role of the charge transfer rather than dipole interaction in the protonation affinity of these compounds.

3.4. Strain energies

Strain energies (Tables 9 and 10) have been estimated from the corresponding homodesmotic reactions (Eq. (1)), at B3LYP/6-311++G(2d,2p), MP2/6-31+G(d), and HF/6-311++G(2d,2p) theoretical levels. For comparison, we also provide in Table 10 the experimental values,[43] together with those recently obtained by Dudev and Lim on the basis of ab initio calculations[44]

$$(CH_2)_nO + 2CH_3\text{–}OH + CH_3\text{–}CH_3 \rightarrow 2CH_3\text{–}CH_2\text{–}OH + CH_3\text{–}O\text{–}(CH_2)_{n-2}\text{–}CH_3 \quad (1)$$

We observe that absolute E_{RS} values are strongly dependent on the computational level. If we focus our attention, however, in relative values we observe a fair agreement between the three sets of values. The negative value of E_{RS} for oxacyclohexane at the HF level suggests the need for electron correlation to obtain reliable energies from homodesmotic reactions. This anomaly was also found to occur in the homodesmotic determination of strain energies in methyl substituted oxacyclopropanes.[11] It is also important to note that oxacyclohexane, often thought as strain-free, possess about 20 kJ mol^{-1} of strain energy, according to both MP2 and B3LYP homodesmotic estimations.

We have also tried to estimate E_{RS} as the difference between the summation of the atomic integrated energies of oxygen and methylenes in the cyclic molecule and those for homologous groups in the open-chain monoether. In all cases, and contrary to what was found in cycloalkanes,[13,17] the calculated values were not in line with those obtained by any of the approaches described above. Why does this method fail? Many reasons can be invoked: (a) the *Z*-dependence displayed by the atomic energies in compounds with highly electronegative atoms precludes direct comparison of atomic energies and obtaining nearly transferable atomic energies, and (b) when E_{RS} is calculated by means of homodesmotic reactions, it is also including the differences between the energy of other groups that do not belong to the cycle and whose molecular environment is meaningfully changed in the process (i.e. CH_3 in ethane and ethanol in Eq. (1)). This fact is also pointed out by the important differences obtained for E_{RS} from the diverse possible homodesmotic processes.[11]

Nevertheless, AIM $E(\Omega)$ and $N(\Omega)$ values provide a description of how the ring formation modifies the properties of each atom. Thus, strain of oxacycloalkanes (as that of

Table 9. Energy (a.u.) and ZPVE (kJ mol^{-1}) for the molecules involved in the evaluation of strain energy from homodesmotic reactions

	B3LYP		HF		MP2	
	E	ZPVE	*E*	ZPVE	*E*	ZPVE
CH_3–OH	−115.77003	134.29	−115.08565	143.93	−115.35784	137.25
CH_3–CH_3	−79.86098	195.61	−79.25700	206.76	−79.497603	201.33
CH_3–CH_2–OH	−155.10176	209.42	−154.13746	223.75	−154.53015	213.99
CH_3–O–CH_3	−155.08371	208.53	−154.11908	222.89	−154.51463	214.7
CH_3–CH_2–O–CH_3	−194.41532	283.06	−193.17083	302.02	−193.68698	290.85
CH_3–$(CH_2)_2$–O–CH_3	−233.74108	357.84	−232.21687	381.45	−232.85377	367.44
CH_3–$(CH_2)_3$–O–CH_3	−273.06694	432.33	−271.26289	406.82	−272.02082	443.71
CH_3–$(CH_2)_2$–O– $(CH_2)_2CH_3$	−312.39825	506.79	−310.31449	539.56	−311.19298	519.64
1			−152.91782	161.66	−153.31481	154.07
2			−191.97097	244.12	−192.48367	232.78
3			−231.04871	327.05	−231.68419	313.36
4			−270.10105	409.54	−270.85903	392.71
5			−309.13199	490.03	−310.01380	470.01

Table 10. Strain energies (kJ mol^{-1}) obtained with homodesmotic reactions

Compound	B3LYP	HF	MP2	Ref. 44	Ref. 43
1	103.98	97.28	110.58	125.52	110.04
2	110.82	89.38	122.22	120.08	103.34
3	33.92	2.19	37.52	33.89	22.59
4	20.51	−18.75	20.07	14.23	0
5	69.20	29.94	67.05	36.40	–

cycloalkanes[13,17]), whatever this quantity is taken to mean, results from a destabilization of oxygen and hydrogens that is not compensated for by the stabilization of cyclic carbons.

4. Concluding remarks

The structural studies of oxacycloalkanes presented here are in good agreement with the available experimental data and also support previous theoretical calculations performed at a lower level of calculation. Concerning oxacyclobutane, the geometrical optimization from a non-planar ring gave a final C_{2v} planar structure, whereas a slightly puckered structure was proposed in a previous X-ray study.

E_{RS} of oxacycloalkanes, as obtained from the homodesmotic approach at the B3LYP and MP2 levels correlate well with those obtained from experimental heats of formation. On the contrary, the HF level does not produce reliable values. The strong inductive effect of oxygen atom on the alkyl chains together with the dependence of atomic energies on the molecular size, prevent us to calculate the E_{RS} from the AIM integrated energies of a related open chain monoether. Strain energy of oxacycloalkanes results from a destabilization of oxygen and hydrogens that is not compensated for by the stabilization of cyclic carbons.

More than 64% of the positive charge resulting from the protonation process is partially concentrated on the proton. Thus, dialkyloxonium cations are better described by an O–H$^+$ structure than by the widespread use of the O$^+$–H structure. The remaining positive charge is dispersed over the hydrogen atoms.

There is a good linear relationship between protonation energies and the charge on the attached proton. It suggests a dominant role of the charge transfer rather than dipole interaction in the protonation affinity of these compounds.

Acknowledgements

This work was partially supported by the Autonomous Government of Galicia. Computer facilities from Centro de Supercomputación de Galicia and stimulating discussions with Diego González at the authors' laboratory are also acknowledged.

References

1. Cremer, D.; Kraka, E. *J. Am. Chem. Soc.* **1985**, *107*, 3800.
2. Cremer, D.; Kraka, E. *J. Am. Chem. Soc.* **1985**, *107*, 3811.
3. Bachrach, S. M. *J. Phys. Chem.* **1989**, *93*, 7780.
4. Alcamí, M.; Mó, O.; Yáñez, M. *J. Comput. Chem.* **1998**, *19*, 1072.
5. Wiberg, K. B.; Márquez, M. *J. Am. Chem. Soc.* **1998**, *120*, 2932.
6. Vila, A.; Carballo, E.; Mosquera, R. A. *Can. J. Chem.* **2000**, *78*, 1535.
7. Vila, A.; Mosquera, R. A. *Chem. Phys. Lett.* **2000**, *332*, 474.
8. Vila, A.; Mosquera, R. A. *J. Phys. Chem. A* **2000**, *104*, 12006.
9. Vila, A.; Mosquera, R. A. *J. Mol. Struct. (Theochem)* **2001**, *546*, 63.
10. Vila, A.; Mosquera, R. A.; Hermida-Ramón, J. M. *J. Mol. Struct. (Theochem)* **2001**, *541*, 149.
11. Vila, A.; Mosquera, R. A. submitted to *J. Chem. Phys.*
12. Bader, R. F. W. *Atoms in Molecules—A Quantum Theory*; *International Series of Monographs on Chemistry*, Vol. 22; Oxford University Press: Oxford, 1990.
13. Bader, R. F. W. *Chem. Rev.* **1991**, *91*, 893.
14. Liebman, J. F.; Greenberg, A. *Chem. Rev.* **1976**, *76*, 311.
15. Franklin, J. L. *Ind. Engng Chem.* **1949**, *41*, 1070.
16. George, P.; Trachtman, M.; Bock, C. W. *Tetrahedron* **1976**, *32*, 317.
17. Wiberg, K. B.; Bader, R. F. W.; Lau, C. D. H. *J. Am. Chem. Soc.* **1987**, *109*, 1001.
18. Frisch, M. J.; Trucks, G. W.; Schlegel, H. B.; Gill, P. M. W.; Johnson, B. G.; Robb, M. A.; Cheeseman, J.R.; Keith, T.; Petersson, G. A.; Montgomery, J. A.; Raghavachari, K.; Al-Laham, M. A.; Zakrzewski, V. G.; Ortiz, J. V.; Foresman, J. B.; Cioslowski, J.; Stefanov, B. B.; Nanayakkara, A.; Challacombe, M.; Peng, C. Y.; Ayala, P. Y.; Chen, W.; Wong, M. W.; Andres, J. L.; Replogle, E. S.; Gomperts, R.; Martin, R. L.; Fox, D. J.; Binkley, S.; Defrees, D. J.; Baker, J.; Stewart, J. P.; Head-Gordon, M.; Gonzalez, C.; Pople, J. A. *Gaussian 94, Revision C.3*, Gaussian, Inc.: Pittsburgh PA, 1995.
19. MORPHY98, a topological analysis program written by P. L. A. Popelier with a contribution from R. G. A. Bone (UMIST, Engl., EU).
20. AIMPAC: A suite of programs for the Theory of Atoms in Molecules; R. F. W. Bader and coworkers Eds., McMaster University, Hamilton, Ontario, Canada, L8S 4M1. Contact bader@mcmail.cis.mcmaster.ca.
21. Aicken, F. M.; Popelier, P. L. A. *Can. J. Chem.* **2000**, *78*, 415.
22. Cadioli, B.; Gallinella, E.; Coulombeau, C.; Jovic, H.; Berthier, G. *J. Phys. Chem.* **1993**, *97*, 7844.
23. Allinger, N. L.; Chung, D. Y. *J. Am. Chem. Soc.* **1976**, *98*, 6798.
24. Espinosa, A.; Gallo, M. A.; Entrena, A.; Gómez, J. A. *J. Mol. Struct.* **1994**, *323*, 247.
25. Luger, P.; Buschmann, J. *J. Am. Chem. Soc.* **1984**, *106*, 7118.
26. Harmony, M. D.; Laurie, V. W.; Kuckzkowski, R. L.; Schewendeman, R. H.; Ramsay, D. A.; Lovas, F. J.; Lafferty, W. J.; Maki, A. G. *J. Phys. Chem. Ref. Data* **1979**, *8*, 619.
27. Geise, H. J.; Adams, W. J.; Bartell, L. S. *Tetrahedron* **1969**, *25*, 3045.
28. Alkorta, I.; Rozas, I.; Elguero *J. Struct. Chem.* **1998**, *9*, 243.
29. Bachrach, S. M. *J. Comput. Chem.* **1989**, *10*, 392.
30. Knop, O.; Boyd, R. J.; Choi, S. C. *J. Am. Chem. Soc.* **1988**, *110*, 7299.
31. Bachrach, S. M. *J. Phys. Chem.* **1989**, *93*, 7780.
32. Coulson, C. A.; Moffitt, W. E. *Philos. Mag.* **1949**, *40*, 1.
33. Graña, A. M.; Mosquera, R. A. *J. Chem. Phys.* **1999**, *110*, 6606.
34. Bader, R. F. W.; Bayles, D. *J. Phys. Chem. A* **2000**, *104*, 5579.

35. Vila, A.; Mosquera, R. A. *J. Chem. Phys.* **2001**, *115*, 1264.
36. Stutchbury, N. C. J.; Cooper, D. L. *J. Chem. Phys.* **1983**, *79*, 4967.
37. Bader, R. F. W. *Can. J. Chem.* **1986**, *64*, 1036.
38. Boys, S. F.; Bernardi, F. *Mol. Phys.* **1970**, *19*, 553.
39. Lias, S. G.; Liebman, J. F.; Levin, R. D. *J. Phys. Chem. Ref. Data* **1984**, *13*, 695.
40. Hunter, E. P.; Lias, S. G. Proton affinity evaluations. NIST Chemistry Webbok; Mallard, W. G., Linstrom, P. J., Eds.; NIST Standard Reference Database Number 69, March 1998; National Institute of Standards and Technology: Gaithersburg MD, 20899 (hhttp://webbook.nist.gov).
41. Nobes, R. H.; Rodwell, W. R.; Bouma, W. J.; Radom, L. *J. Am. Chem. Soc.* **1981**, *103*, 1913.
42. Abboud, J. L. M.; Elguero, J.; Liotard, D.; Essefard, M. H.; Mouthadi, M. E.; Taft, R. W. *J. Chem. Soc. Perkin Trans. 2* **1990**, 565.
43. Eigenmann, H. K.; Golden, D. M.; Benson, S. W. *J. Phys. Chem.* **1973**, *77*, 1687.
44. Dudev, T.; Lim, C. *J. Am. Chem. Soc.* **1998**, *120*, 4450.